IEEE Access
Multidisciplinary | Rapid Review | Open Access Journal

Received September 9, 2020, accepted September 21, 2020, date of publication September 23, 2020,
date of current version October 2, 2020.

Digital Object Identifier 10.1109/ACCESS.2020.3026205

String Stability Analysis of Mixed CACC Vehicular Flow With Vehicle-to-Vehicle Communication

YANYAN QIN AND SHUQING LI
School of Traffic and Transportation, Chongqing Jiaotong University, Chongqing 400074, China

Corresponding author: Yanyan Qin (qinyanyan@cqjtu.edu.cn)

This work was supported by the National Key Research and Development Program in China under Grant 2018YFB1601000.

ABSTRACT This paper focuses on traffic scenarios randomly mixed with cooperative adaptive cruise control (CACC) vehicles and manual vehicles with vehicle-to-vehicle (V2V) communication. The analytical investigation of string stability of such mixed traffic flow is conducted under different CACC penetration rates. The parametric sensitivity analysis on CACC desired time-gap is also studied. Moreover, numerical simulation is conducted under both open and periodic boundary conditions. Research results indicate that increase of CACC vehicles is helpful for improving the mixed traffic flow string stability. The mixed flow will be stable for all possible velocities if CACC rate reaches to 0.64 when the CACC time-gap is considered as 0.6s. Larger CACC time-gap would have more stable regions in string stability charts with respect to equilibrium velocity and CACC penetration rate. This paper contributes to a new way for analytical investigation of string stability of the mixed CACC traffic flow.

INDEX TERMS Cooperative adaptive cruise control, string stability, mixed traffic flow, numerical simulations.

I. INTRODUCTION

String stability is an important topic in research of traffic flow dynamics [1]–[5]. It depicts how a perturbation propagates to vehicles upstream with time. To avoid ambiguity, we should mention that string stability studied in this paper is also called asymptotic stability in traffic flow modeling [6]. In recent years, vehicle intelligent systems, such as cooperative adaptive cruise control (CACC), are developed to improve traffic flow dynamics [7]. Theoretically speaking, CACC can monitor multiple vehicles ahead with vehicle-to-vehicle (V2V) communication. However, the real experiments [8], [9] indicate that the CACC vehicle might only receive information from the immediately preceding vehicle, which serves the first step toward multiple V2V communication at the present stage. Therefore, this paper focuses on the CACC vehicle that monitors the immediately preceding vehicle. Moreover, like some previous studies [10], [11], manual vehicles are assumed to be able to send their diving information to CACC vehicles using V2V communication devices, regardless of whether they can receive information from other vehicles or not.

The associate editor coordinating the review of this manuscript and approving it for publication was Guangdeng Zong.

A special designed microscopic simulation model was employed to show that CACC vehicles contribute to stability of traffic flow [12]. The macroscopic model for CACC traffic flow dynamics was also developed from gas-kinetic theory [13], and it was found that CACC enhances string stability of traffic flow with respect to both small and large perturbations. In addition, some CACC controller implementations in production vehicles were performed [14]. These tests indicate that CACC vehicle can improve string stability and provide valuable experience for bringing CACC control technologies into production [9]. However, a relationship has yet to be established between these control technologies [15], [16] and car-following models for the investigation under different CACC penetration rates. Therefore, a car-following model of the CACC control system implemented in real vehicles was developed based on experiments [8], [9]. The results show that CACC vehicles can smooth perturbation waves, but this literature did not analyze string stability in detail with different CACC penetration rates. Since market penetration level of CACC vehicles will increase gradually over a long period of times, the future traffic flow will be randomly mixed with manual vehicles and CACC vehicles. Such mixed traffic flow is likely to be realistic in the near future and its string stability becomes importation topic in traffic flow theory. Many studies [17]–[34] have been conducted to analyze the

impacts of CACC vehicles on traffic flow stability. From the perspective of analytical investigation, we found that there are two major approaches for analytical investigation of string stability of the mixed traffic flow in the previous studies. The framework by Ward [24] focusing on car-truck mixed flow was successfully extended to the mixed CACC traffic flow [35]–[38]. However, Ward's framework [24] cannot directly deal with the string stability conditions, in which the reaction time is considered. To deal with this problem, transfer function theory is applied to stability analysis of the mixed CACC traffic scenario [36]. The shortcoming of this method is that the reaction time would make transfer function substantially more complicated. Therefore, it needs a relative simple method to calculate string stability of the mixed CACC traffic flow by taking into consideration the reaction time. Fortunately, from the perspective of anticipation time and reaction time with respect to perturbation waves, Holland [23] studied string stability of both identical and non-identical drivers. Additionally, his string stability criterion was successfully applied to determine conditions required by stable traffic flow on the M25 in the U.K [23]. However, to the best of our knowledge, Holland' method [23] has not been extended to the case of the mixed CACC flow. Therefore, this article attempts to address this case by analytically investigating string stability of the mixed CACC traffic flow.

The remainder of this paper is organized as follows. In Section II, car-following models of CACC and manual vehicles are described. Then analytical investigation of string stability is conducted in Section III. Section IV performs numerical simulations under both open and periodic boundary conditions. Finally, conclusions are summarized in Section V.

II. CAR-FOLLOWING MODELS

A. MANUAL DRIVEN MODEL

Newell investigated a car-following model with velocity governing equation in 1961 [39]. The Newell model is written as

$$v_i(t+T) = V(x_{i-1}(t) - x_i(t)) \tag{1}$$

where T is time lag, x_{i-1} and x_i are positions of the preceding and following vehicles, v_i is the velocity of vehicle i, V is the optimal velocity function.

In 1995, Bando *et al.* presented the optimal velocity model (OVM), a breakthrough of car-following models [40]:

$$\dot{v}_i(t) = \gamma[V(x_{i-1}(t) - x_i(t)) - v_i(t)] \tag{2}$$

where $\dot{v}_i$ stands for the acceleration of vehicle i, γ is sensitivity parameter, which means the reaction time of OVM is considered as $1/\gamma$ [41].

Then, the generalized force model (GFM) [42] was proposed to solve the problems of high accelerations and decelerations in OVM. After that, Jiang *et al.* [43] modified the GFM model by considering both positive and negative velocity difference, called the full velocity difference model (FVDM):

$$\dot{v}_i(t) = \kappa[V(x_{i-1}(t) - x_i(t)) - v_i(t)] + \lambda(v_{i-1}(t) - v_i(t)) \tag{3}$$

TABLE 1. Calibration results of FVDM.

Parameters	Values
v_0	18.1 m/s
κ	0.204 s^{-1}
l	5.23 m
β	2.14 m
λ	0.536 s^{-1}
λ	18.1 m/s

where κ and λ are sensitivity parameters. The optimal velocity function V used by Kesting and Treiber [44] is adopted in this paper in order to use their parameter calibration results, which is written as

$$V = \frac{v_0}{2}[\tanh(\frac{x_{i-1} - x_i}{l} - \beta) - \tanh(-\beta)] \tag{4}$$

where v_0 is desired velocity, l and β determine the transition regime for V.

The parameter values of FVDM were calibrated by Kesting and Treiber [44] using trajectory data of daily city traffic. The calibration results are shown in Table 1. Because the desired velocity is calibrated to be 18.1 m/s in daily city traffic, the mixed traffic flow studied by this paper is supposed to run under this desired velocity value.

B. CACC MODEL

PATH proposed a CACC model by simplifying a CACC controller implemented in production vehicles [8], [9]. The CACC controller is divided into gap closing stage and gap regulation stage [9]. This paper focuses on string stability analysis, which requires the initial state to be stable. Therefore, only the gap regulation stage is employed as the CACC model, which is calculated as follows:

$$v_i = v_{iprev} + k_p e_i + k_d \dot{e}_i \tag{5}$$

where v_{iprev} is the velocity of following vehicle in the previous iteration, k_p and k_d are control gains, e_i denotes the gap distance error, and $\dot{e}_i$ is the derivative of e_i about time. The e_i is calculated as follows:

$$e_i = x_{i-1} - x_i - t_c v_i \tag{6}$$

where t_c is the CACC time-gap, which ranges from 0.6s to 1.1s [45].

The values of k_p and k_d are determined based on the CACC implementation [8], [9], where $k_p = 0.45$ and $k_d = 0.25$. The experimental tests show that the CACC model properly matches the real behavior of the production vehicles equipped with this CACC control system.

III. ANALYTICAL INVESTIGATION OF STRING STABILITY

A. ANALYTICAL GUIDELINES

String stability studies the propagation of perturbation along the platoon over time. If the perturbation is gradually attenuated when propagating upstream, the platoon is called string stable. As mentioned previously, only a few literatures including the one by Holland [23] studied the string stability of the mixed traffic flow. We adopt the finding of Holland's study to analyze the string stability situations with respect

to equilibrium velocities and CACC penetration rates for the mixed CACC traffic flow.

Based on Holland [23], the car-following dynamics can be interpreted from the perspective of wave travel times and reaction times. By introducing the idea of an anticipation point [23] and considering the fact that perturbations are likely to be smoothed out when propagating along a column for stable traffic flow [39], [46], [47], Holland [23] calculated a diffusion coefficient as the string stability criterion for the mixed traffic flow as follows,

$$f = \frac{1}{N}\sum_{i=1}^{N}[\tau_i(\alpha_i\tau_i - T_i)] \tag{7}$$

where f is the diffusion coefficient and traffic flow is stable if its value is positive. i denotes the ith vehicle in the traffic flow containing N vehicles. α_i is the anticipation point, τ_i is the time that a wave takes to travel between two adjacent vehicles, and T_i is the reaction time.

According to Holland [23], the string stability criterion in Eq. (7) does not depend on the orders of individual vehicles. Moreover, the reaction time T_i can be explicitly manifested as a direct time lag, such as Newell model in Eq. (1), and also implicitly as an expression of the sensitivity parameters, such as OVM in Eq. (2). The anticipation point α_i is proved to be 1/2 if the car-following model is based on spatial headway or velocity difference [23]. The wave travel time τ_i is derived by Holland [23] as follows:

$$\tau_i = [V_i'(b)]^{-1} \tag{8}$$

where $V_i(b)$ is the equilibrium velocity-headway function of the ith vehicle's car-following law, and b denotes the equilibrium spatial headway.

Based on Holland [23], it means the ith driver have enough time to react to the wave before it reaches him/her if the term $(\tau_i\ (\alpha_i\tau_i - T_i))$ is positive. The physical interpretation of the diffusion coefficient f is how much the perturbation waves are diffused in total as it passes down the column [23]. In addition, Eq. (7) will become the string stability criterion for homogenous car-following models when drivers follow the same law:

$$f_Q = \tau(\alpha\tau - T) \tag{9}$$

where subscript Q denotes vehicle type. The traffic flow is stable if f_Q is positive.

B. HOMOGENOUS TRAFFIC FLOW

1) MANUAL VEHICLES

In this section, the string stability of homogenous traffic flow is analyzed based on Eq. (9). In the case of manual vehicles, the car-following model is FVDM introduced by Eq. (3). We rewrite its string stability criterion, i.e. Eq. (9), as follows,

$$f_Q = \tau(\alpha\tau - T) \tag{10}$$

where, subscript m denotes manual vehicles. Because the car-following law of FVDM is based on spatial headway and velocity difference, the value of α_m is 1/2 [23]. FVDM can be derived from general Newell model as the second-order expression [41], based on which the relation time of FVDM is calculated as

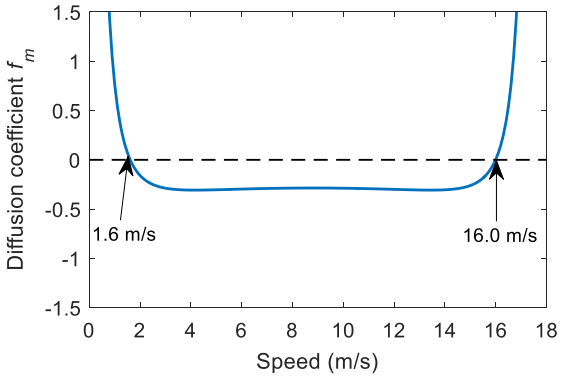

FIGURE 1. String stability of manual vehicles.

$$T_m = \frac{1}{\kappa + 2\lambda} \tag{11}$$

where, κ and λ are sensitivity parameters of FVDM, whose values are shown in Table 1. Therefore, the value of T_m is calculated to be 0.78s.

At the equilibrium state, the acceleration and velocity difference are zeros. For FVDM, the equilibrium velocity-headway function is the optimal velocity function of Eq. (4). Hence, its wave travel time is obtained, as follows,

$$\tau_m = [V_m'(b)]^{-1} = \frac{2l}{v_0[1 - (\tanh(\frac{b}{l} - \beta))^2]} \tag{12}$$

Based on the optimal velocity function of FVDM, b can be written as the function of the equilibrium velocity:

$$b = l[\arctan h[\frac{2v}{v_0} + \tanh(-\beta)] + \beta] \tag{13}$$

where v is the equilibrium velocity.

Substituting Eq. (13) to Eq. (12) to rewrite τ_m as follows:

$$\tau_m = \frac{2l}{v_0[1 - \tanh^2(\arctan h(\frac{2v}{v_0} + \tanh(-\beta)))]} \tag{14}$$

Substituting Eq. (11), Eq. (14), and $\alpha_m = 1/2$ into Eq. (10) to obtain the diffusion coefficient f_m of manual vehicles, as follows,

$$f_m = \frac{2l^2}{v_0^2[1 - \tanh^2(\arctan h(\frac{2v}{v_0} + \tanh(-\beta)))]^2} - \frac{2l}{v_0(\kappa + 2\lambda)[1 - \tanh^2(\arctan h(\frac{2v}{v_0} + \tanh(-\beta)))]} \tag{15}$$

Eq. (15) shows that the values of f_m are determined only by equilibrium velocities once values of model parameters are determined. It means the string stability of manual vehicles is determined by equilibrium velocities, as shown in Fig. 1. It shows that f_m is positive when the equilibrium velocity is below 1.6 m/s or over 16.0 m/s (the desired velocity is calibrated as 18.1 m/s), while negative if the velocity ranges between 1.6 m/s and 16.0 m/s. Thus, manual vehicles are

stable when the velocity ranges from 0 m/s to 1.6 m/s and from 16.0 m/s to 18.1 m/s, while unstable if the velocity changes between 1.6 m/s and 16.0 m/s.

2) CACC VEHICLES

In the case of CACC vehicles, the string stability criterion for homogenous traffic flow, i.e. Eq. (9), is rewritten as,

$$f_c = \tau_c(\alpha_c \tau_c - T_c) \tag{16}$$

where, c denotes the CACC vehicle type. Based on this CACC control principle [8], [9], the CACC model, i.e. Eq. (5), can be replaced by

$$v_i(t + \Delta t) = v_i(t) + k_p e_i(t) + k_d \dot{e}_i(t) \tag{17}$$

where, Δt is the control cycle, which is 0.01s during experimental tests [8], [9]. In other words, the reaction time T_c of actual CACC vehicles is 0.01s. Because the CACC model is also based on spatial headway and velocity difference, the value of α_c is 1/2 [23].

Substituting the equilibrium state conditions into CACC model to obtain its velocity-headway function:

$$V_c(b) = \frac{b}{t_c} \tag{18}$$

Hence, the wave travel time of CACC vehicles is obtained as follows:

$$\tau_c = [V_c'(b)]^{-1} = t_c \tag{19}$$

Therefore, the diffusion coefficient f_c of CACC vehicles can be calculated based on Eq. (16), as follows,

$$f_c = \frac{1}{2} t_c^2 - t_c \Delta t \tag{20}$$

Eq. (20) indicates that f_c is only determined by CACC model and does not depend on vehicle velocities. Based on the CACC model used in this paper, the value of f_c can be calculated to be 0.1740. It means CACC vehicles are stable for any velocity.

C. MIXED TRAFFIC FLOW

In the previous section, we calculate the diffusions of manual vehicles and CACC vehicles, which are denoted by f_m and f_c in Eq. (15) and Eq. (20), respectively. Then following Eq. (7), the diffused perturbation wave in total for a column can be calculated by summing the diffusion for each vehicle when the wave passes through it. Moreover, the calculation does not depend on the orders of individual vehicles but on the numbers of different types of vehicles [23]. Let p_m and p_c denote the proportions of manual vehicles and CACC vehicles, respectively, in the mixed traffic flow. Moreover, let p stand for the CACC penetration rate, which means $p_m = 1-p$ and $p_c = p$. Then Eq. (7) can be extended to the mixed CACC traffic flow studied in this paper:

$$f_t = p_m f_m + p_c f_c = (1-p) f_m + p f_c \tag{21}$$

where, f_t denotes the total diffusions, namely the diffusion coefficient in Eq. (7).

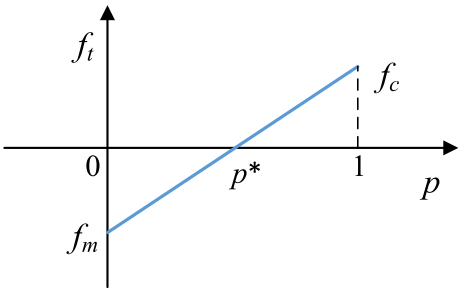

FIGURE 2. Function of f_t related to p.

In order to explore quantitative relationship between total diffusions f_t and p, we transfer Eq. (21) to the function of f_t related to p, as follows:

$$f_t = (f_c - f_m)p + f_m \tag{22}$$

It can be found that f_t is a linear function about p. Moreover, the value of f_t is f_m when p is 0, while it is f_c if p increases to 1. According to the above analysis, f_c is positive and the values of f_m depend on equilibrium velocities. Hence, we can categorize conditions into the following two general cases. The first case means $f_m \geq 0$. Then f_t is always positive based on properties of linear function. In this case, the mixed traffic would be stable for each possible value of p. The second case denote $f_m < 0$. In this case, f_t would be negative when p is 0, while it is positive when p is 1, as shown in Fig. 2, in which the line stands for the quantitative relationship between f_t and p. We can calculate each value of f_t based on values of p. Moreover, f_t would be changed from negative values to positive values when p reaches p^*. According to the linear function, we can calculate the quantitative values of p^*, as follows:

$$p^* = \frac{f_m}{f_m - f_c} \tag{23}$$

By substituting Eq. (15) and Eq. (20) into Eq. (23), we can calculate the values of f_t under different CACC penetration rates and equilibrium velocities. Then the mixed traffic flow string stability charts with respect to CACC penetration rates and equilibrium velocities can be obtained, as shown in Fig. 3. The black curve denotes values of p^*, calculated according to Eq. (23), depending on equilibrium velocities. Then the mixed traffic flow is unstable for the area below the black curve, while the region above stands for stable situations. The intersections of the black curve and the horizontal axis with 0% CACC rate are 1.6 m/s and 16.0 m/s, which are critical velocities between stability and instability of manual vehicles. What we mainly concern are the critical CACC rates that can maintain stable mixed traffic flow under each velocity, which are the values on the black curve in Fig. 3. According to the string stability charts with various values of CACC time-gap, it shows that larger CACC time-gap decrease the corresponding critical CACC rates. It can be calculated that the mixed traffic flow will become stable for all velocities when the CACC rate p is more than 0.64, in the case of CACC time-gap being 0.6s. If the CACC time-gap

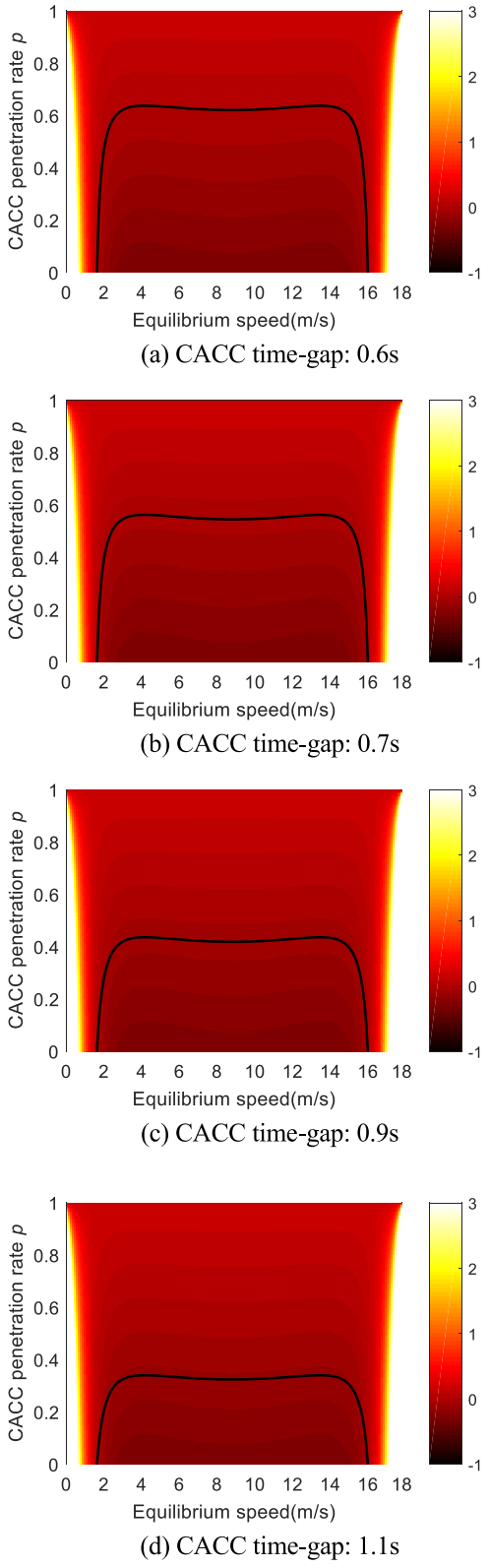

FIGURE 3. String stability charts of the mixed CACC traffic flow.

is 0.7s, the stable mixed flow can be obtained when CACC rate p reaches to 0.56, while the corresponding critical CACC rate is 0.44 in the case of CACC time-gap being 0.9s. In addition, if CACC time-gap increases to 1.1s, the mixed traffic flow can satisfy the string stability with more than 0.34 rate of CACC.

As noted in the introduction section, previous studies [35]–[38] usually adopted the method by Ward [24] and the method of transfer function theory [36] to conduct string stability of the mixed CACC flow. However, Ward's method cannot deal with the reaction time well. Hence, from the perspective of reaction time, the method used in this paper is more useful for analytical investigation of string stability of the mixed CACC traffic flow. In addition, although transfer function theory has the ability to analyze the reaction time of string stability, the reaction time would make the calculation substantially complicated. Moreover, the reaction time would also cause transcendental equation. The final analytical criterion of string stability cannot be obtained, while numerical computation is usually adopted to calculate the stability results of the mixed traffic with CACC vehicles [36]. Therefore, compared with the method of transfer function theory, our method is actually practical to deal with string stability of the mixed CACC flow when reaction times of vehicles are considered. Moreover, the method used in this paper has less computational cost.

IV. NUMERICAL SIMULATIONS

String stability analysis in section 3 belongs to the linear stability. However, except for very abstract models, non-linear string stability analysis is not analytically tractable for mixed traffic flow [36], [37]. Therefore, we perform numerical simulations to evaluate string stability at the non-linear level by using car-following models. The simulations are conducted under both open and periodic boundary conditions.

A. SIMULATIONS UNDER OPEN BOUNDARY CONDITION

The numerical simulations under open boundary condition focus on a mixed platoon containing 50 vehicles. The leading vehicle is controlled and performs a deceleration to cause a small perturbation. Specifically, at the initial time, all vehicles of the platoon travel at equilibrium velocity 10m/s. Then the leading vehicle decelerates its velocity with the deceleration -0.5m/s^2 for 2s to maintain a new constant velocity until the end of simulations [48]. Then we evaluate the time history of vehicle velocities for the string stability analysis. The simulations are performed using Matlab, a computational software package. In the simulations, car-following dynamics of manual and CACC vehicles are achieved by using their car-following model described in section 2. Because small value of CACC time gap may help increase traffic capacity, the CACC time gap is set to be 0.6s in simulations. We focus on the mixed traffic flow with different CACC penetration rates, which means the mixed platoon in simulations containing manual and CACC vehicles. The proportions of manual and CACC vehicles in the mixed platoon are determined by the value of CACC penetration rates, which is set in advance in the procedure using Matlab. Moreover, the vehicle orders in the mixed platoon are also random on the single lane. The simulation time step is 0.1s.

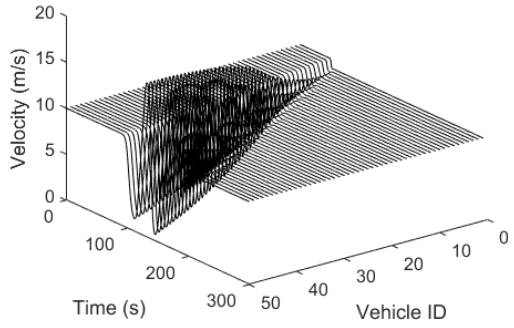

(a) CACC penetration rate p=0

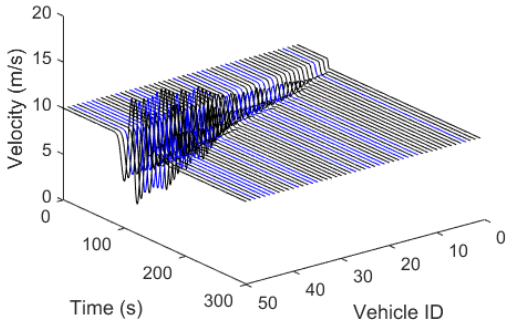

(b) CACC penetration rate p=0.3

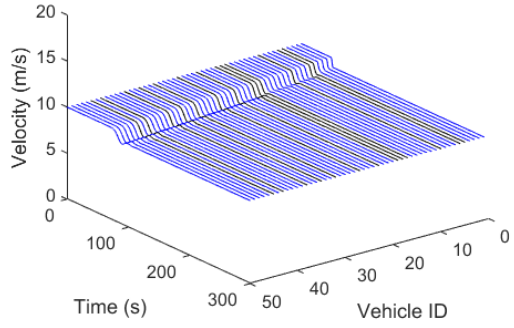

(c) CACC penetration rate p=0.7

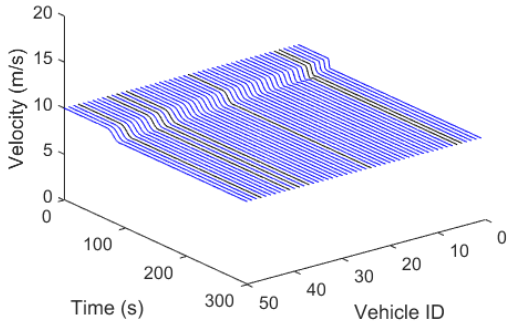

(d) CACC penetration rate p=0.8

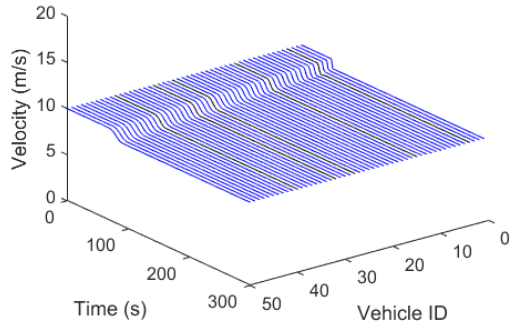

(e) CACC penetration rate p=0.9

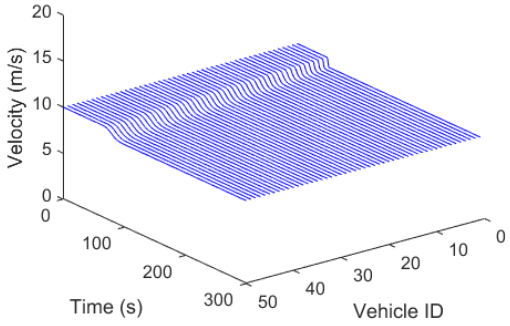

(f) CACC penetration rate p=1

FIGURE 4. Simulation results under open boundary condition.

Based on the above simulation designs, the simulation results are shown in Fig. 4. In Fig. 4, the blue curves denote velocity dynamics of CACC vehicles, while the black curves represent the velocity dynamics of manual vehicles. Fig. 4 gives non-linear string stability results with six CACC penetration rates. It can be found that manual vehicles are unstable under the small perturbation caused by the leading vehicle. The string stability of the mixed platoon is gradually improved with the increase of the CACC penetration rate p. When p researches to 0.8, the mixed platoon becomes stable. Therefore, the critical value of p that maintains stable platoon ranges from 0.7 to 0.8. As noted previously in Fig. 3 (a), in the linear analytical level, the critical value of p for stable mixed traffic flow is 0.64. Then the difference between linear analytical result and non-linear simulation result is not significant, which also validates the analytical investigation in this paper.

In order to further evaluate how the stability changes by CACC penetration rates, we conduct statistical test to analyze whether there are significant changes. As for simulations under open boundary condition, shown in Fig. 4, speed

TABLE 2. Velocity amplitude comparison with CACC penetration rates.

CACC rate	Velocity amplitude of five vehicles ID (m/s)				
p	ID: 10	ID: 20	ID: 30	ID: 40	ID: 50
0	1.1571	2.7901	5.5052	7.3072	8.2749
0.1	0.9488	2.2125	4.9774	7.0638	8.1749
0.2	0.9486	1.9435	3.6298	5.8367	7.4672
0.3	0.9478	1.7001	2.6066	5.1694	7.0129
0.4	0.4330	1.4760	1.8050	3.6787	5.3638
0.5	0.1782	0.5966	1.6042	1.9520	3.1379
0.6	0.1776	0.4675	0.7485	0.8966	1.0439
0.7	0.0798	0.1663	0.1703	0.2157	0.7056
0.8	0.0127	0.0944	0.1605	0.1741	0.2158
0.9	0.0018	0.0033	0.0036	0.0078	0.0403
1.0	1.76E-10	1.76E-10	1.77E-10	1.77E-10	1.77E-10

TABLE 3. Statistical significant of velocity amplitude.

CACC rate p	P-value
0	/ (base line)
0.1	# 0.8674
0.2	# 0.5793
0.3	# 0.4119
0.4	# 0.1639
0.5	# 0.0405
0.6	# 0.0123
0.7	# 0.0078
0.8	# 0.0066
0.9	# 0.0058
1.0	# 0.0056

Note: #Difference is insignificant at the 5% level.

changes of vehicles over time are illustrated. Then we can calculate maximum amplitude of a certain vehicle's velocities over time, which is compared with the equilibrium velocity. We select five vehicles to conduct this comparison, whose vehicles ID is 10, 20, 30, 40, and 50, respectively. The calculation results are shown in Table 2. Based on the results in Table 2, the two-sample t-test at 5% significance level [49] is used as the statistical test. When we make the t-test, the velocity amplitude with full manual vehicles (namely $p = 0$) is considered as the base line. Then cases with different CACC penetration rates are tested and results are calculated in Table 3. According to Table 3, It can be found that P-values decrease with the increase of CACC penetration rate p. Moreover, we can find that improvements of string stability will be significant when p increases to 0.5. This shows the usefulness that CACC vehicles enhance stability conditions of the mixed traffic flow.

B. SIMULATIONS UNDER PERIODIC BOUNDARY CONDITION

Besides the open boundary condition, periodic boundary condition is useful to evaluate snapshots of vehicle velocities of the platoon with different CACC penetration rates. Therefore, we also conducted numerical simulations under periodic boundary condition. The simulations under periodic boundary condition are also performed in Matlab with the simulation time step being 0.1s. At the initial time, all vehicles (also 50 vehicles) have the same velocity 10m/s and move on a single-lane ring road in steady state, in which the distance gap of each manual vehicle is 13.8881m and each CACC vehicle's distance gap is 8m. The vehicle orders are also random under

TABLE 4. Velocity variance comparison with CACC penetration rates.

CACC rate	Velocity variance at time t (m/s)^2				
p	t=100	t=300	t=500	t=700	t=900
0	40.0364	57.4322	57.1222	57.2524	57.3960
0.1	38.2139	55.2991	55.4486	55.8198	55.8502
0.2	35.9606	53.3167	53.3901	54.7927	54.6902
0.3	31.2895	52.5245	52.9352	53.2808	53.7671
0.4	30.5511	47.9592	47.4156	47.2133	47.4222
0.5	24.6639	44.4351	45.6089	45.2579	46.0264
0.6	18.3863	34.2007	38.2258	38.5378	38.4893
0.7	15.0081	20.4201	24.7168	32.5518	34.5110
0.8	1.0037	1.0114	1.0492	1.2126	1.8486
0.9	0.0231	0.0619	0.0119	0.0226	0.0422
1.0	1.60E-06	1.30E-12	1.06E-18	3.96E-25	3.91E-25

TABLE 5. Statistical significant of velocity variance.

CACC rate p	P-value
0	/ (base line)
0.1	# 0.7345
0.2	# 0.5144
0.3	# 0.3878
0.4	# 0.0791
0.5	# 0.0470
0.6	# 0.0045
0.7	# 4.83E-04
0.8	# 3.44E-04
0.9	# 2.87E-07
1.0	# 2.85E-07

Note: #Difference is insignificant at the 5% level.

periodic boundary condition. A small perturbation is added onto one of the vehicles to see how the perturbation develops along the platoon [5], [22]. Simulations are also conducted under six different CACC penetration rates, namely $p = 0$, 0.3, 0.7, 0.8, 0.9, 1. The snapshots of vehicle velocities at the time step of $t = 300$s are shown in Fig. 5. In the case of full manual vehicles, i.e. $p = 0$, the perturbation causes stop-and-go phenomenon under periodic boundary condition. This stop-and-go phenomenon can be gradually removed with the increase of the CACC penetration rate p. Moreover, when p reaches 0.8, the mixed platoon would become stable on the single-lane ring road. Hence, the string stability performance under the periodic boundary condition (Fig. 5) is consistent with that under the open boundary condition (Fig. 4).

As for the simulations under periodic boundary condition, we also test statistical significant of stability conditions of the mixed vehicular flow. In Fig. 5, snapshots of vehicle velocities at a certain time are illustrated. Then velocity variances of all vehicles at a certain time are calculated under different CACC penetration rate p. We select $t = 100$s, $t = 300$s, $t = 500$s, $t = 700$s, and $t = 900$s in the statistical test. According to the above consideration, calculation results of velocity variance are shown in Table 4. The condition of velocity variance with $p = 0$ is also considered as the base line in the statistical test, in which two-sample t-test at 5% significance level [49] is still used. Results of statistical significant are calculated in Table 5. Based on results of Table 5, P-value also decreases with the increase of p under the periodic boundary condition. Moreover, enhancement of stability conditions of the mixed flow will be significant if

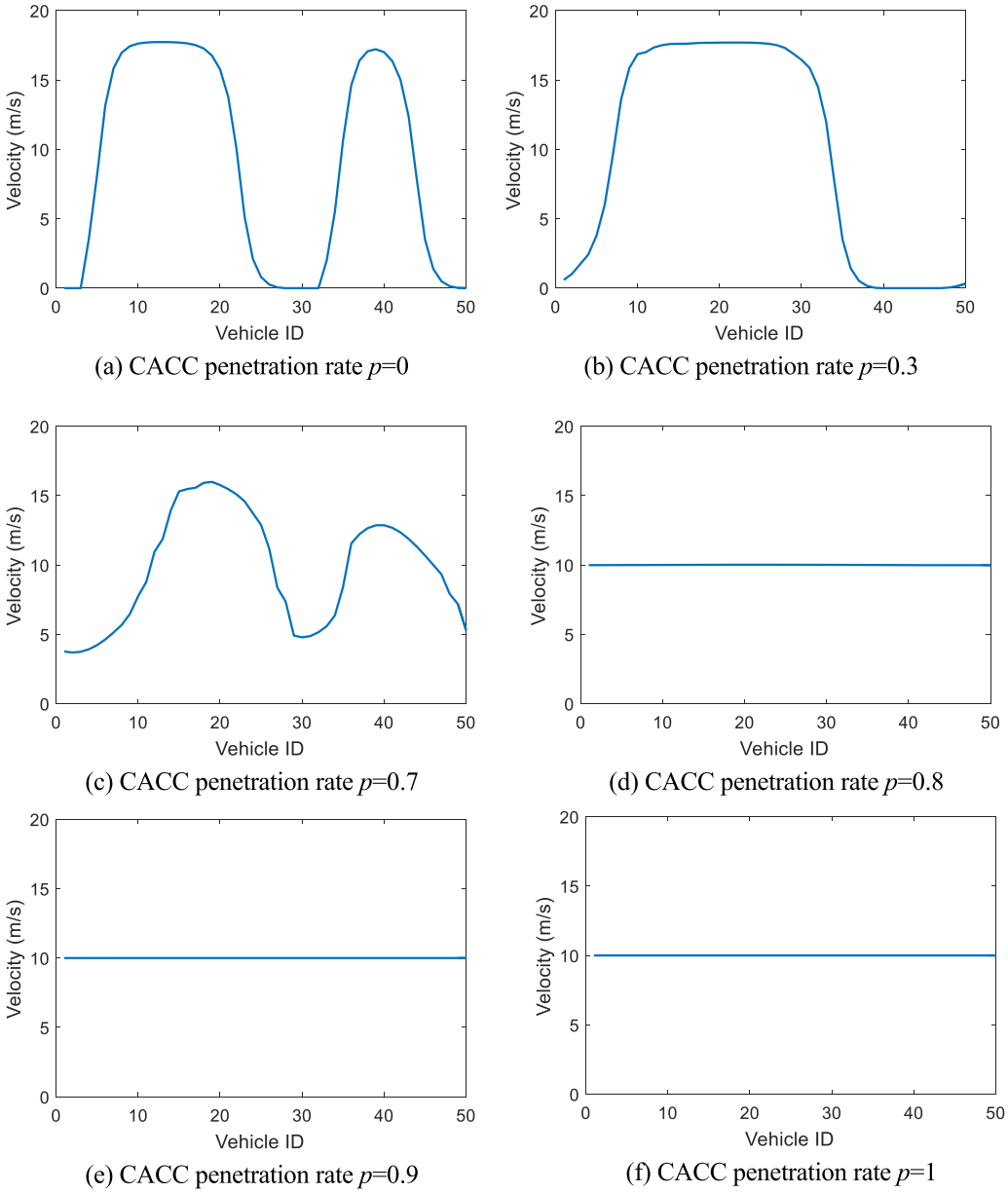

FIGURE 5. Snapshots of vehicle velocities at the time step of t = 300s.

p increases to 0.5, which is consistent with results in Table 3 under the open boundary condition. This means that the usefulness of stability enhancement by CACC vehicles in the mixed flow is also validated based on the periodic boundary condition.

V. CONCLUSION

This paper focuses on string stability of the mixed CACC traffic flow with V2V communication. Although this mixed traffic flow is likely to be realistic in the near future, analytical investigation of its string stability is not fully studied. Therefore, we analytically investigate the string stability of this mixed traffic flow, by extending the analytical guidelines proposed by Holland [23]. Conclusions are obtained under the assumption that the future factory CACC system is based on the CACC controller implemented in production vehicles [8], [9]. It shows that CACC vehicles are helpful in improving string stability of the mixed traffic flow. Larger time-gap of this CACC controller have larger stable regions of the string stability chart with respect to equilibrium velocities and CACC penetration rates. When CACC time-gap is set to be 0.6s, the mixed traffic flow will be stable for all velocities if the CACC penetration rate exceeds 0.64, while the critical CACC penetration rate is required to be more than 0.34 if CACC time-gap is considered as 1.1s.

The study in this paper provides a new way for string stability analysis of the mixed CACC traffic flow. The analytical framework presented for the investigation of string stability can be applied to the case in which CACC model are improved for better description of car-following dynamics

of real vehicles in the future. Additionally, the presented analytical framework can be applied to various spatial traffic scenarios, if calibration works of manual driven model are performed using corresponding trajectory data. Although numerical simulations are performed to validate the analytical results in this paper, we are aware that empirical data are still not available, which will be left in our next research step when large-scale experimental data of CACC vehicles are available in the future. In addition, stochastic noises and structure switches widely exist in the real word [50]–[52]. Hence, the effect of stochastic noises and structure switches will be further considered in the future.

ACKNOWLEDGMENT

The authors would like to thank the anonymous reviewers for reviewing this article.

REFERENCES

[1] M. Wang, S. P. Hoogendoorn, W. Daamen, B. van Arem, B. Shyrokau, and R. Happee, "Delay-compensating strategy to enhance string stability of adaptive cruise controlled vehicles," *Transportmetrica B, Transp. Dyn.*, vol. 6, no. 3, pp. 211–229, Jul. 2018.

[2] Z. Li, R. Zhang, S. Xu, Y. Qian, and J. Xu, "Stability analysis of dynamic collaboration model with control signals on two lanes," *Commun. Nonlinear Sci. Numer. Simul.*, vol. 19, no. 12, pp. 4148–4160, Dec. 2014.

[3] G. Peng, D. Xia, and S. Yang, "The stability of traffic flow on two lanes incorporating Driver's characteristics corresponding to honk effect under V2X environment," *IEEE Access*, vol. 8, pp. 73879–73889, Apr. 2020.

[4] Y.-Y. Qin, Z.-Y. He, and B. Ran, "Rear-end crash risk of CACC-manual driven mixed flow considering the degeneration of CACC systems," *IEEE Access*, vol. 7, pp. 140421–140429, 2019.

[5] K. Ma and H. Wang, "Influence of exclusive lanes for connected and autonomous vehicles on freeway traffic flow," *IEEE Access*, vol. 7, pp. 50168–50178, 2019.

[6] J. Sun, Z. Zheng, and J. Sun, "Stability analysis methods and their applicability to car-following models in conventional and connected environments," *Transp. Res. B, Methodol.*, vol. 109, pp. 212–237, Mar. 2018.

[7] S. E. Shladover, C. Nowakowski, X.-Y. Lu, and R. Ferlis, "Cooperative adaptive cruise control: Definitions and operating concepts," *Transp. Res. Rec., J. Transp. Res. Board*, vol. 2489, no. 1, pp. 145–152, Jan. 2015.

[8] V. Milanés and S. E. Shladover, "Modeling cooperative and autonomous adaptive cruise control dynamic responses using experimental data," *Transp. Res. C, Emerg. Technol.*, vol. 48, pp. 285–300, Nov. 2014.

[9] V. Milanes, S. E. Shladover, J. Spring, C. Nowakowski, H. Kawazoe, and M. Nakamura, "Cooperative adaptive cruise control in real traffic situations," *IEEE Trans. Intell. Transp. Syst.*, vol. 15, no. 1, pp. 296–305, Feb. 2014.

[10] J. I. Ge and G. Orosz, "Dynamics of connected vehicle systems with delayed acceleration feedback," *Transp. Res. C, Emerg. Technol.*, vol. 46, pp. 46–64, Sep. 2014.

[11] J. I. Ge, S. S. Avedisov, C. R. He, W. B. Qin, M. Sadeghpour, and G. Orosz, "Experimental validation of connected automated vehicle design among human-driven vehicles," *Transp. Res. C, Emerg. Technol.*, vol. 91, pp. 335–352, Jun. 2018.

[12] B. van Arem, C. J. G. van Driel, and R. Visser, "The impact of cooperative adaptive cruise control on traffic-flow characteristics," *IEEE Trans. Intell. Transp. Syst.*, vol. 7, no. 4, pp. 429–436, Dec. 2006.

[13] D. Ngoduy, "Instability of cooperative adaptive cruise control traffic flow: A macroscopic approach," *Commun. Nonlinear Sci. Numer. Simul.*, vol. 18, no. 10, pp. 2838–2851, Oct. 2013.

[14] E. van Nunen, M. R. J. A. E. Kwakkernaat, J. Ploeg, and B. D. Netten, "Cooperative competition for future mobility," *IEEE Trans. Intell. Transp. Syst.*, vol. 13, no. 3, pp. 1018–1025, Sep. 2012.

[15] A. Geiger, M. Lauer, F. Moosmann, B. Ranft, H. Rapp, C. Stiller, and J. Ziegler, "Team AnnieWAY's entry to the 2011 grand cooperative driving challenge," *IEEE Trans. Intell. Transp. Syst.*, vol. 13, no. 3, pp. 1008–1017, Sep. 2012.

[16] L. Guvenc, I. M. C. Uygan, K. Kahraman, R. Karaahmetoglu, I. Altay, M. Senturk, M. T. Emirler, A. E. Hartavi Karci, B. Aksun Guvenc, E. Altug, M. C. Turan, Ö. S. Tas, E. Bozkurt, Ü. Ozguner, K. Redmill, A. Kurt, and B. Efendioglu, "Cooperative adaptive cruise control implementation of team mekar at the grand cooperative driving challenge," *IEEE Trans. Intell. Transp. Syst.*, vol. 13, no. 3, pp. 1062–1074, Sep. 2012.

[17] H. S. Mahmassani, "50th anniversary invited Article—Autonomous vehicles and connected vehicle systems: Flow and operations considerations," *Transp. Sci.*, vol. 50, no. 4, pp. 1140–1162, Jun. 2016.

[18] K. Konishi, H. Kokame, and K. Hirata, "Decentralized delayed-feedback control of an optimal velocity traffic model," *Eur. Phys. J. B*, vol. 15, no. 4, pp. 715–722, Jun. 2000.

[19] J. Sau, J. Monteil, R. Billot, and N.-E. El Faouzi, "The root locus method: Application to linear stability analysis and design of cooperative car-following models," *Transportmetrica B, Transp. Dyn.*, vol. 2, no. 1, pp. 60–82, Apr. 2014.

[20] T.-Q. Tang, H.-J. Huang, and Z.-Y. Gao, "Stability of the car-following model on two lanes," *Phys. Rev. E, Stat. Phys. Plasmas Fluids Relat. Interdiscip. Top.*, vol. 72, no. 6, Dec. 2005, Art. no. 066124.

[21] A. Kesting and M. Treiber, *Traffic Flow Dynamics: Data, Models and Simulation*. Berlin, Germany: Springer, 2013.

[22] R. E. Wilson, "Mechanisms for spatio-temporal pattern formation in highway traffic models," *Phil. Trans. Roy. Soc. A, Math., Phys. Eng. Sci.*, vol. 366, no. 1872, pp. 2017–2032, Jun. 2008.

[23] E. N. Holland, "A generalised stability criterion for motorway traffic," *Transp. Res. B, Methodol.*, vol. 32, no. 2, pp. 141–154, Feb. 1998.

[24] J. A. Ward, "Heterogeneity, lane-changing and instability in traffic: A mathematical approach," M.S. thesis, Univ. Bristol, Bristol, U.K., 2009.

[25] A. Talebpour, H. S. Mahmassani, and A. Elfar, "Investigating the effects of reserved lanes for autonomous vehicles on congestion and travel time reliability," *Transp. Res. Rec., J. Transp. Res. Board*, vol. 2622, no. 1, pp. 1–12, Jan. 2017.

[26] Y. Zhou, S. Ahn, M. Chitturi, and D. A. Noyce, "Rolling horizon stochastic optimal control strategy for ACC and CACC under uncertainty," *Transp. Res. C, Emerg. Technol.*, vol. 83, pp. 61–76, Oct. 2017.

[27] M. Wang, "Infrastructure assisted adaptive driving to stabilise heterogeneous vehicle strings," *Transp. Res. C, Emerg. Technol.*, vol. 91, pp. 276–295, Jun. 2018.

[28] X. Sun and Y. Yin, "Behaviorally stable vehicle platooning for energy savings," *Transp. Res. C, Emerg. Technol.*, vol. 99, pp. 37–52, Feb. 2019.

[29] Y. Qin, H. Wang, and B. Ran, "Impacts of cooperative adaptive cruise control platoons on emissions under traffic oscillation," *J. Intell. Transp. Syst.*, pp. 1–8, Dec. 2019, doi: 10.1080/15472450.2019.1702534.

[30] Y. Zhou, M. Wang, and S. Ahn, "Distributed model predictive control approach for cooperative car-following with guaranteed local and string stability," *Transp. Res. B, Methodol.*, vol. 128, pp. 69–86, Oct. 2019.

[31] D. Liu, Z. Shi, and W. Ai, "An improved car-following model accounting for impact of strong wind," *Math. Problems Eng.*, vol. 2017, Oct. 2017, Art. no. 4936490.

[32] T. Zhou, D. Chen, L. Zheng, W. Liu, Y. He, and Z. Liu, "Feedback-based control for coupled map car-following model with time delays on basis of linear discrete-time system," *Phys. A, Stat. Mech. Appl.*, vol. 512, pp. 174–185, Dec. 2018.

[33] S. Jin, D.-H. Sun, M. Zhao, Y. Li, and J. Chen, "Modeling and stability analysis of mixed traffic with conventional and connected automated vehicles from cyber physical perspective," *Phys. A, Stat. Mech. Appl.*, vol. 551, Aug. 2020, Art. no. 124217.

[34] A. Talebpour, H. S. Mahmassani, and S. H. Hamdar, "Effect of information availability on stability of traffic flow: Percolation theory approach," *Transp. Res. B, Methodol.*, vol. 117, pp. 624–638, Nov. 2018.

[35] D. Ngoduy, "Effect of the car-following combinations on the instability of heterogeneous traffic flow," *Transportmetrica B, Transp. Dyn.*, vol. 3, no. 1, pp. 44–58, Jan. 2015.

[36] Y. Qin and H. Wang, "Analytical framework of string stability of connected and autonomous platoons with electronic throttle angle feedback," *Transportmetrica A, Transp. Sci.*, pp. 1–22, Sep. 2018, doi: 10.1080/23249935.2018.1518964.

[37] A. Talebpour and H. S. Mahmassani, "Influence of connected and autonomous vehicles on traffic flow stability and throughput," *Transp. Res. C, Emerg. Technol.*, vol. 71, pp. 143–163, Oct. 2016.

[38] D. Ngoduy, "Linear stability of a generalized multi-anticipative car following model with time delays," *Commun. Nonlinear Sci. Numer. Simul.*, vol. 22, nos. 1–3, pp. 420–426, May 2015.

[39] G. F. Newell, "Nonlinear effects in the dynamics of car following," *Oper. Res.*, vol. 9, no. 2, pp. 209–229, Apr. 1961.
[40] M. Bando, K. Hasebe, A. Nakayama, A. Shibata, and Y. Sugiyama, "Dynamical model of traffic congestion and numerical simulation," *Phys. Rev. E, Stat. Phys. Plasmas Fluids Relat. Interdiscip. Top.*, vol. 51, no. 2, pp. 1035–1042, Feb. 1995.
[41] H. Wang, W. Wang, and J. Chen, "General newell model and related second-order expressions," *Transp. Res. Rec., J. Transp. Res. Board*, vol. 2260, no. 1, pp. 42–49, Jan. 2011.
[42] D. Helbing and B. Tilch, "Generalized force model of traffic dynamics," *Phys. Rev. E, Stat. Phys. Plasmas Fluids Relat. Interdiscip. Top.*, vol. 58, no. 1, pp. 133–138, Jul. 1998.
[43] R. Jiang, Q. Wu, and Z. Zhu, "Full velocity difference model for a car-following theory," *Phys. Rev. E, Stat. Phys. Plasmas Fluids Relat. Interdiscip. Top.*, vol. 64, no. 1, Jun. 2001, Art. no. 017101.
[44] A. Kesting and M. Treiber, "Calibrating car-following models by using trajectory data: Methodological study," *Transp. Res. Rec., J. Transp. Res. Board*, vol. 2088, no. 1, pp. 148–156, Jan. 2008.
[45] S. E. Shladover, D. Su, and X.-Y. Lu, "Impacts of cooperative adaptive cruise control on freeway traffic flow," *Transp. Res. Rec., J. Transp. Res. Board*, vol. 2324, no. 1, pp. 63–70, Jan. 2012.
[46] R. E. Chandler, R. Herman, and E. W. Montroll, "Traffic dynamics: Studies in car following," *Oper. Res.*, vol. 6, no. 2, pp. 165–184, Apr. 1958.
[47] R. Herman, E. W. Montroll, R. B. Potts, and R. W. Rothery, "Traffic dynamics: Analysis of stability in car following," *Oper. Res.*, vol. 7, no. 1, pp. 86–106, Feb. 1959.
[48] H. Wang, Y. Qin, W. Wang, and J. Chen, "Stability of CACC-manual heterogeneous vehicular flow with partial CACC performance degrading," *Transportmetrica B, Transp. Dyn.*, vol. 7, no. 1, pp. 788–813, Dec. 2019.
[49] Y. Qin and H. Wang, "Influence of the feedback links of connected and automated vehicle on rear-end collision risks with vehicle-to-vehicle communication," *Traffic Injury Prevention*, vol. 20, no. 1, pp. 79–83, Feb. 2019.
[50] G. Zong, W. Qi, and H. R. Karimi, "Lü control of positive semi-Markov jump systems with state delay," *IEEE Trans. Syst., Man, Cybern. Syst.*, early access, Mar. 24, 2020, doi: 10.1109/TSMC.2020.2980034.
[51] G. Zong, H. Ren, and H. R. Karimi, "Event-triggered communication and annular finite-time H_∞ filtering for networked switched systems," *IEEE Trans. Cybern.*, early access, Aug. 7, 2020, doi: 10.1109/TCYB.2020.3010917.
[52] T. Jiao, W. X. Zheng, and S. Xu, "Unified stability criteria of random nonlinear time-varying impulsive switched systems," *IEEE Trans. Circuits Syst. I, Reg. Papers*, vol. 67, no. 9, pp. 3099–3112, Sep. 2020.

YANYAN QIN received the Ph.D. degree in transportation engineering from Southeast University, Nanjing, China, in 2019. He is currently an Assistant Professor with the School of Traffic and Transportation, Chongqing Jiaotong University, since 2019. His research interests include intelligent transportation systems, traffic flow theory, and impacts of connected vehicles on traffic safety.

SHUQING LI received the B.Eng. degree in highway engineering from Southeast University, Nanjing, China, in 1983, and the master's degree in transportation engineering from Tongji University, Shanghai, China, in 1989. He is currently a Professor with Chongqing Jiaotong University. He is also the Assistant Dean of the School of Traffic and Transportation, Chongqing Jiaotong University. His research interests include transportation planning and design, traffic capacity, and safety evaluation.